Int. J. Heat Mass Transfer. Vol. 30, No. 5, pp. 1007–1015, 1987
Printed in Great Britain

0017–9310/87 $3.00 + 0.00

Flow and mass transfer characteristics in wavy channels for oscillatory flow

TATSUO NISHIMURA, ATSUSHI TARUMOTO and YUJI KAWAMURA
Department of Chemical Engineering, Hiroshima University, Higashi-Hiroshima, Japan 724

(*Received* 9 *May* 1986 *and in final form* 3 *September* 1986)

Abstract—A study of fluid flow and mass transfer for oscillatory flow has been carried out in wavy channels, which consist of two sinusoidal wavy plates. The experiments were carried out under the following conditions: $5 \times 10^2 < Re_p < 10^4$, $2.1 \times 10^{-2} < St_p < 8.6 \times 10^{-2}$. The flow was neither dominated by viscous forces nor quasi-steady in this experiment. The recirculation vortex is formed within the furrow during the acceleration phase and is ejected from the wall just after flow reversal. The mass transfer rate strongly depends on Re_p, but the effect of St_p is insignificant. The wavy channels yield a large mass transfer enhancement as compared with the corresponding straight channel. This enhancement is attributed to the vortex ejection observed.

1. INTRODUCTION

BELLHOUSE *et al.* [1] have developed a high-efficiency membrane oxygenator which utilizes pulsatile flow through a wavy channel to achieve high mass transfer rates. However, it is not obvious under what conditions and to what extent mass transfer enhancement will take place.

In order to explain the mechanism of this mass transfer enhancement, Sobey [2] numerically analyzed the oscillatory flow in a sinusoidal wavy channel for laminar flow. He presented periodic changes in the streamlines and suggested that a recirculation vortex formation/ejection induced by the oscillatory flow was responsible for the enhanced mass transfer. Furthermore, Stephanoff *et al.* [3] supported the calculated flow patterns of Sobey by the flow observations. However, the study of mass transfer has not been performed yet.

Nishimura *et al.* [4–7] studied analytically and experimentally the steady fluid flow and mass transfer in several channels with a sinusoidal wavy wall in the laminar and turbulent flow regimes. It was found that a significant mass transfer enhancement was not recognized except for the turbulent flows regime, as compared with the corresponding straight channel. Also Aggarwal and Talbot [8] measured mass transfer rates in a single semi-cylindrical hollow under steady laminar flow conditions as a simple model of the membrane oxygenator of Bellhouse *et al.* The mass transfer results obtained fell below those for the straight channel. So it is necessary that the previous studies are extended to the unsteady flow case to evaluate the effect of unsteady flow on the mass transfer in the laminar flow regime.

In this study we experimentally observed the flow behavior and measured the mass transfer rates in unsteady flow in the same wavy channels as those previously used. Oscillatory flow was considered as the unsteady flow. Because the membrane oxygenator of Bellhouse *et al.* is operated under pulsatile flow close to oscillatory flow, i.e. a mean flow of less than one-tenth the peak flow. Furthermore, the mass transfer comparisons between the wavy channel and the corresponding straight channel were carried out to assess the effectiveness of the wavy channel as a mass transfer device.

2. EXPERIMENTAL APPARATUS

A schematic diagram of the experimental apparatus is shown in Fig. 1. Flow oscillations were produced by a Scotch-yoke-driven piston/cylinder arrangement. The volumetric flow rate was measured using an electromagnetic flow meter and it was sinusoidal ($Q_i = 2\pi fs(\pi D^2/4) \sin(2\pi ft)$). The ranges of variables investigated in this experiment are given in Table 1.

The wavy channel consisted of two sinusoidal wavy plates which could be misaligned by some angle ϕ. The mean spacing between two wavy plates was 13 mm, yielding the cross-sectional aspect ratio of 15.38. Each wavy plate had an amplitude-to-length ratio $2a/\lambda$ of 0.25 and ten crests separated by a distance of 28 mm. The channels of three geometries ($\phi = 0$, 90° and 180°) were employed as shown in the upper part of Fig. 2. The wavy channel for $\phi = 180°$ has a geometry similar to that of the membrane oxygenator of Bellhouse *et al.* [1]. The straight channel identical with the wavy channel, e.g. equal spacing between the walls and aspect ratio were also used to examine the enhancement provided by the wavy channel as shown in the lower part of Fig. 2.

3. EXPERIMENTAL PROCEDURE

The flow patterns were visualized by the aluminum dust method. Perfusion with a suspension of alumi-

NOMENCLATURE

a wave amplitude of wavy wall [m]
D diameter of piston [m]
D_h hydraulic diameter for straight channel [m]
F molecular diffusivity [$m^2 s^{-1}$]
f frequency of flow rate [s^{-1}]
H_{av} average spacing between wavy walls [m]
H_{min} minimum spacing between walls [m]
k mass transfer coefficient [$m s^{-1}$]
L mass transfer length [m]
Q_i instantaneous volumetric flow rate [$m^3 s^{-1}$]
Q_p peak flow rate, $2\pi fs(\pi D^2/4)$ [$m^3 s^{-1}$]
Re_p peak Reynolds number, $U_p H_{av}/\nu$ [—]
Re^* peak Reynolds number defined by Sobey, $U_p^* H_{min}/2\nu$ [—]
Re_h peak Reynolds number defined by Ohmi *et al.*, $U_m D_h/\nu$ [—]
s stroke of piston [m]
Sc Schmidt number [—]
Sh_i instantaneous Sherwood number, kH_{av}/F [—]
Sh_p maximum Sherwood number [—]
Sh_v mininum Sherwood number [—]
$\overline{Sh}$ time-averaged Sherwood number [—]
Sh_s Sherwood number for straight channel [—]
Sh_w Sherwood number for wavy channel [—]
St_p Strouhal number, $\alpha^2/Re_p = \omega H_{av}/U_p$ [—]
St^* Strouhal number defined by Sobey, $fH_{min}/(2U_p^*)$ [—]
T duration of time, $1/f$ [s]
t time [s]
U_p peak velocity based on H_{av}, $Q_p/(H_{av}W)$ [$m s^{-1}$]
U_p^* peak velocity based on H_{min}, $Q_p/(H_{min}W)$ [$m s^{-1}$]
U_m peak velocity for straight channel [$m s^{-1}$]
W width of wavy wall [m].

Greek symbols

α Womersley number, $H_{av}\sqrt{(\omega/\nu)}$ [—]
α_h Womersley number defined by Ohmi *et al.*, $(D_h/2)\sqrt{(\omega/\nu)}$ [—]
λ wavelength of wavy wall [m]
ν kinematic viscosity [$m^2 s^{-1}$]
ϕ phase difference between upper and lower wavy walls [deg]
ω angular frequency, $2\pi f$ [s^{-1}].

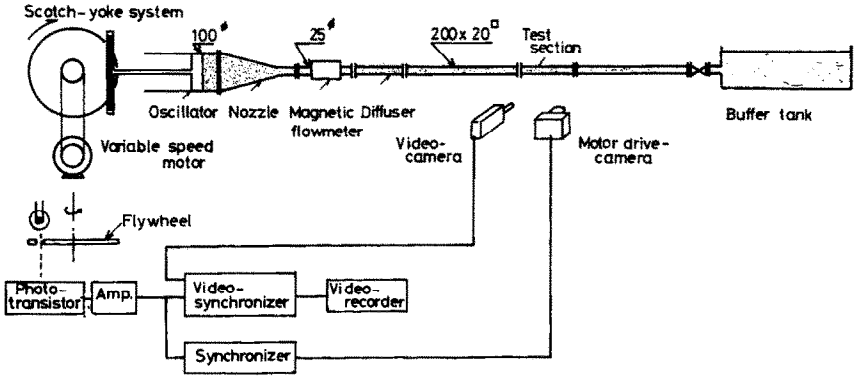

FIG. 1. Flow system.

num particles, about 40 μm in diameter, enabled us to observe streak lines within the whole flow field. City water was the fluid used. Visualized flow patterns were photographed by a video-camera and the motor-driven camera were electrically triggered by the pulse of a photo-transistor as shown in the lower part of Fig. 1.

The mass transfer rates were measured by the electrochemical method, which can be applied to the unsteady flow [9–11]. Three wavy cathodes consisting of nickel-plated brass (L/λ = 1, 2 and 3) were used to determine the effect of the length of the mass transfer section. These cathodes were located in the middle part of the lower wavy plate as shown in Fig. 3. The upper wavy plate, made of nickel-plated brass, was used for the anode. The area ratio of anode to cathode was from 20.8 to 41.6. In addition, the flat cathodes were employed for the straight channel. The electrolyte solution used contained 0.01 N potassium ferri-ferro cyanide and 1.0 N sodium hydroxide. The details of the procedure have been described in previous studies [5, 6] for the steady flow case.

The experiments were made by changing the frequency and strokes of the piston: $5\times10^2 < Re_p < 10^4$, $2.1\times10^{-2} < St_p < 8.6\times10^{-2}$, where Re_p is proportional to a product of the frequency and the stroke, and St_p is inversely proportional to the stroke only.

Table 1. Characteristics of oscillator

Diameter of piston	10 cm
Stroke of piston	5–20 cm
Time period	3–30 s
Maximum flow rate	82–3288 $cm^3\ s^{-1}$

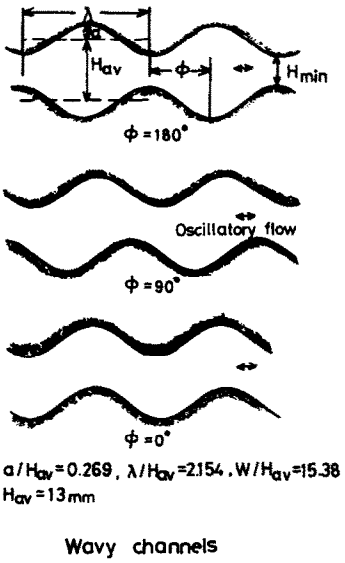

FIG. 2. Types of channels.

4. RESULTS AND DISCUSSION

4.1. *Flow pattern in wavy channels*

The flow patterns scarcely change in this experimental range. Figure 4 shows a schematic diagram of the periodic change in the flow pattern for $\phi = 180°$. Early in the acceleration phase $(t_1 - t_2)$, the flow separation occurs slightly downstream from the minimum cross-section, forming a recirculation vortex and then the separated flow region or the vortex expands rapidly. After that $(t_2 - t_3)$, the extent of the separated flow region becomes almost constant, but a fluid mixing as observed in the steady turbulent flow regime

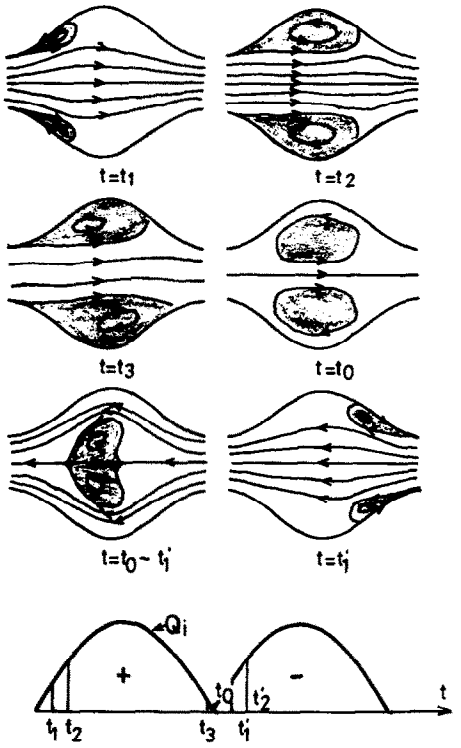

FIG. 4. Schematic flow patterns for wavy channel of $\phi = 180°$.

[4, 6] occurs between the mainstream and the separated flow region due to the vorticity concentration of the separated shear layer. At the end of the deceleration phase $(t_3 - t_0)$, the separated flow region or the vortex does not decrease in size, as happens in quasi-steady flow, but expands gradually over the entire flow region in each section per unit wavelength. As the main flow reverses $(t_0 - t_1')$, the fluid now moves between the vortex and the wall, ejecting the vortex into the mainstream. The process of the ejection occurs at a short time $((t_1' - t_0)/T < 0.05)$. Figure 5 shows the photographs of the flow pattern at $Re_p = 2440$ and $St_p = 8.61 \times 10^{-2}$ as an example. The vortex formation and ejection are observed from path lines of aluminum particles.

As mentioned above, Sobey [2] numerically analyzed oscillatory flow in a sinusoidal wavy channel at lower Reynolds numbers than those considered herein. The dimensions of the channel $(a/H_{av} = 0.25$ and $\lambda/H_{av} = 2.0)$ are slightly different from those of the channel used in this study $(a/H_{av} = 0.269$ and

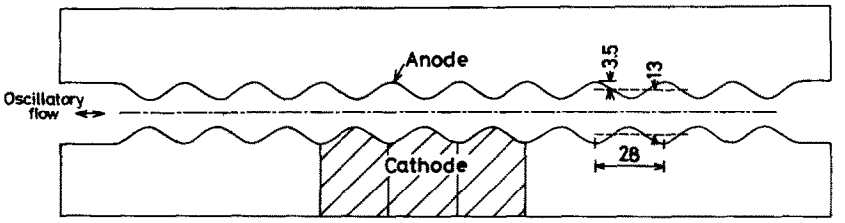

FIG. 3. Details of test section and positions of electrodes.

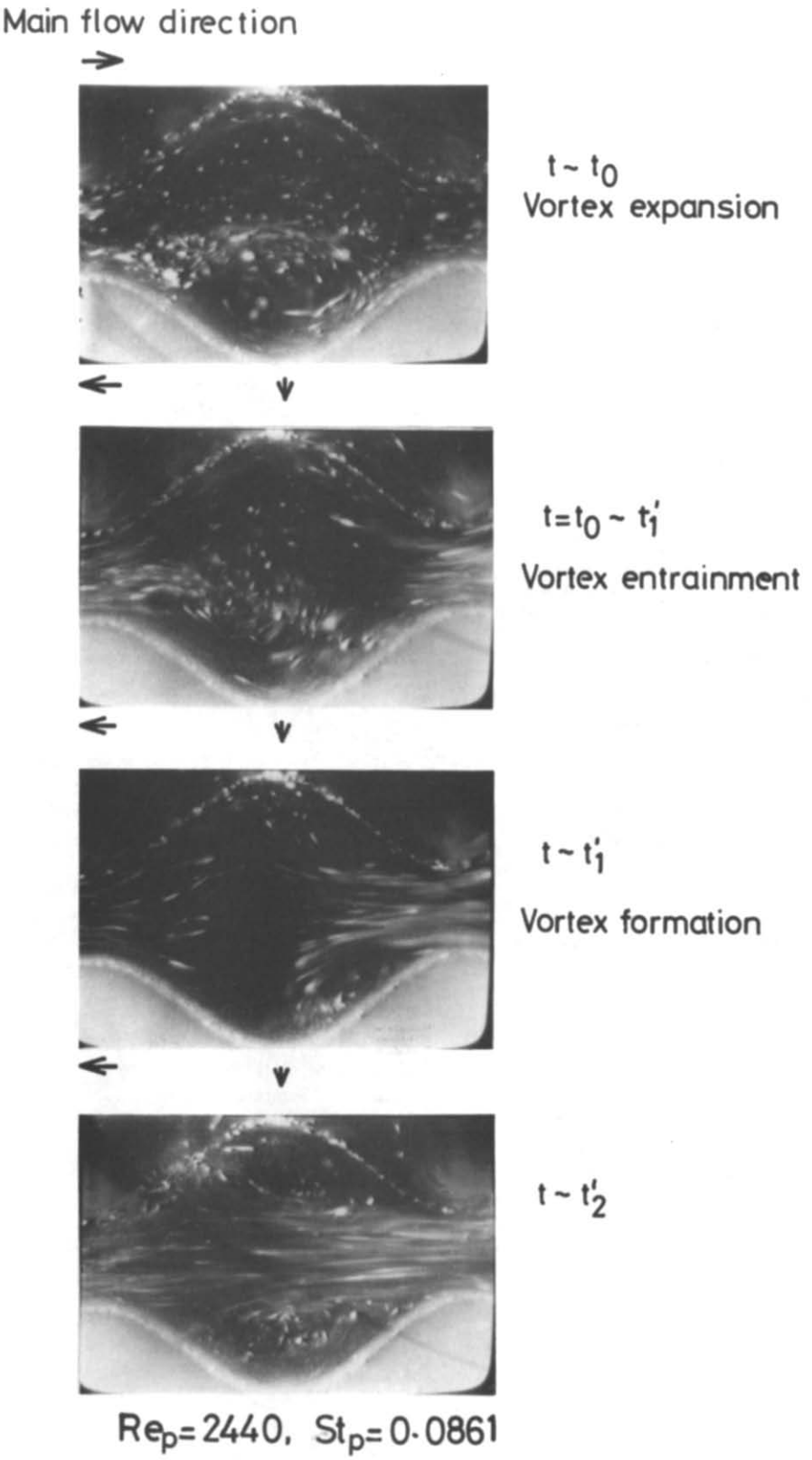

FIG. 5. Photographs of flow pattern for wavy channel of $\phi = 180°$.

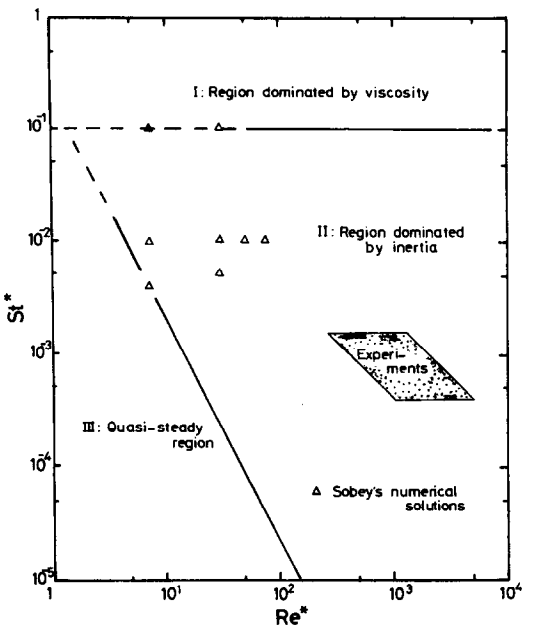

FIG. 6. Flow diagram for wavy channel of $\phi = 180°$ proposed by Sobey.

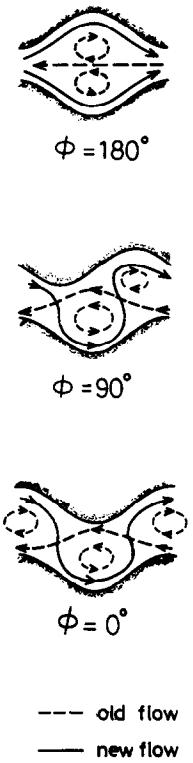

FIG. 7. Schematic flow patterns before and after flow reversal for wavy channels.

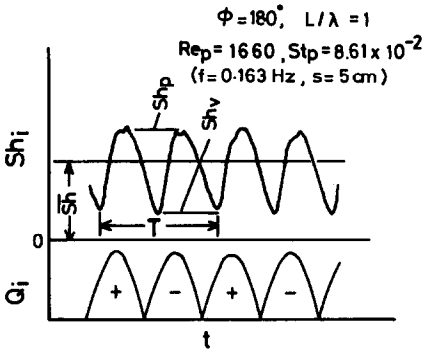

FIG. 8. Time variation of Sherwood number.

$\lambda/H_{av} = 2.154$), but this difference seems to be minute. Sobey defined two flow regions of viscous dominance and inertial dominance for the variation of the Reynolds number, Re^*, and the Strouhal number, St^*. Furthermore, he [12] extended the previous study and presented the flow diagram in a wide range of Reynolds and Strouhal numbers as shown in Fig. 6, which gives guidelines for the boundaries of three regions. This diagram was confirmed by the numerical results at low Reynolds numbers ($Re^* < 75$). Our experimental conditions are included into the region dominated by inertia as also shown in this figure. The flow patterns observed herein are similar to those calculated in the region dominated by inertia at low Reynolds numbers by Sobey [2, 12] and thus the basic flow property such as the vortex ejection is maintained regardless of the magnitude of the Reynolds and Strouhal numbers, if the flow condition is fixed in the region dominated by inertia. However, near the peak flow rate some turbulence appears due to an instability of the separated shear layer, indicating that the flow in this experimental range does not behave in laminar motion wholly because of higher Reynolds numbers, in contrast to the case of Sobey.

Next we briefly discuss how the process of vortex formation and ejection is affected by the variation of ϕ. The flow property observed in the channel for $\phi = 180°$ exists in other channels for $\phi = 0$ and 90°, but the detail of vortex ejection occurring just after reversal of the main flow is different. Figure 7 shows schematic diagrams of the flow pattern for three channels before and after flow reversal. The vortices no longer appear in pairs adjacent to each other in the cases of $\phi = 0$ and 90°. This means that when the main flow reverses, the fluid passes between the two vortices, forming a high convoluted path, in contrast to the case of $\phi = 180°$.

4.2. *Mass transfer in wavy channels*

Figure 8 shows the variation of the instantaneous Sherwood number with time as an example. The Sherwood number periodically varies with time, but its variation is slightly different from that of the volumetric flow rate in a sinusoidal form. Namely the increasing rate of Sherwood number in the acceleration phase is larger than the decreasing rate in the

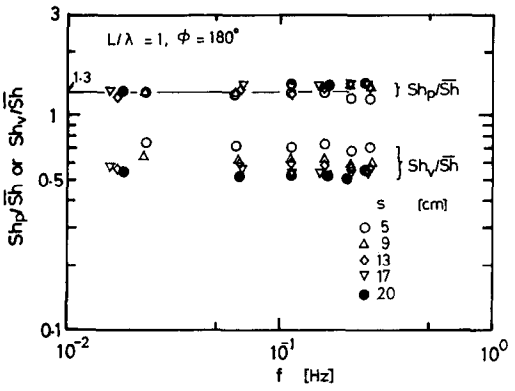

FIG. 9. $Sh_p/\overline{Sh}$ or $Sh_v/\overline{Sh}$ vs f.

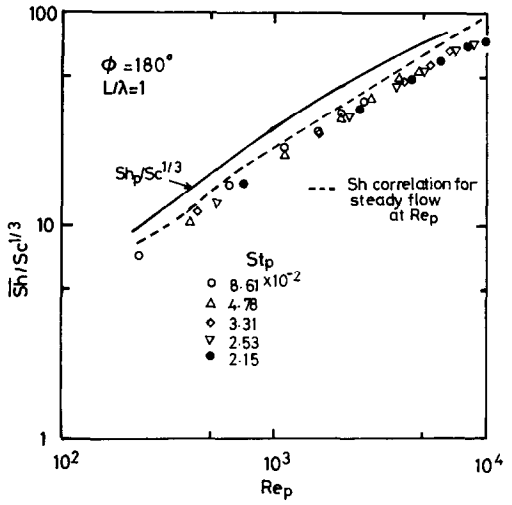

FIG. 10. $\overline{Sh}$ vs Re_p for wavy channel of $\phi = 180°$.

deceleration phase. The Sherwood number also has a phase lag referred to the flow rate. These characteristics were qualitatively the same for other conditions in this experimental range.

We call $\overline{Sh}$, Sh_p and Sh_v represented in this figure time-averaged Sherwood number, maximum Sherwood number and minimum Sherwood number, respectively. Figure 9 shows the relationship between the Sherwood number ratio of $Sh_p/\overline{Sh}$ or $Sh_v/\overline{Sh}$ and the frequency of the piston. Both Sherwood number ratios are almost independent of the frequency of the piston, but the effect of the stroke of the piston appears in $Sh_v/\overline{Sh}$. This behavior indicates that the ratio of the amplitude of instantaneous Sherwood number to the time-averaged Sherwood number is larger for a larger stroke.

The time-averaged Sherwood number is an important factor in the design of mass transfer devices, and it depends on four parameters for the oscillatory flow: Re_p, St_p, Sc and L/λ. Figure 10 shows the relationship between the Sherwood number and the Reynolds number at $L/\lambda = 1$ and $\phi = 180°$. The ordinate of this figure is represented by $Sh/Sc^{1/3}$, because the Sherwood number is proportional to $Sc^{1/3}$ which is confirmed by the additional experiments ($Sc = 1500 \sim 3000$). The Sherwood number strongly depends on the Reynolds number, but the effect of the Strouhal number is insignificant in this experiment.

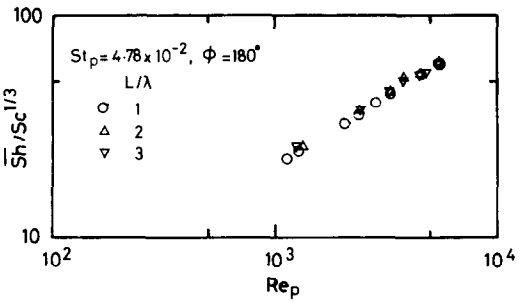

FIG. 11. Effect of L/λ on $\overline{Sh}$.

The dotted line also shown in this figure is the correlation for the steady flow corresponding to the Reynolds number at the peak flow rate of oscillatory flow [5, 6]. The solid line denotes the correlation of the maximum Sherwood number for the oscillatory flow, which scarcely depends on the Strouhal number as well as the time-averaged Sherwood number correlation. From the comparison of these two correlations, it is identified that the effect of oscillatory flow on the mass transfer enhancement is positive.

The effect of mass transfer length was insignificant in this experimental range ($L/\lambda = 1, 2$ and 3) as shown in Fig. 11, and thus the Sherwood number for even $L/\lambda = 1$ can be regarded as the fully developed value. The reason for this is that the concentration boundary layer is destroyed by the vortex ejection as observed by the flow visualizations and it is periodically developed in each section per unit wavelength. This characteristic was also shown for the steady turbulent flow case, but this reason is due to an instability of the separated shear layer [4–7].

These characteristics were the same for other wavy channels for $\phi = 0$ and 90°, and the Sherwood numbers were almost equal to each other, regardless of different processes of vortex ejection as mentioned above, which is shown in Fig. 12.

4.3. *Fluid flow and mass transfer in straight channel*

Flow studies have been numerous. Ohmi *et al.* [13] recently proposed a generalized flow diagram which represents three flow regions of laminar, transitional and turbulent flows in a wide range of Reynolds and Womersley numbers based on a hydraulic diameter, Re_h and α_h, as shown in Fig. 13. The flow diagram indicated that the flow patterns in this experiment were included into three flow regions. This was additionally confirmed by the flow visualizations. We observed that some turbulence was induced during the deceleration phase in the turbulent flow region.

Very little is known about the mass transfer for oscillatory flow, so we investigated the mass transfer for the straight channel. Figure 14 shows the relationship between the time-averaged Sherwood number

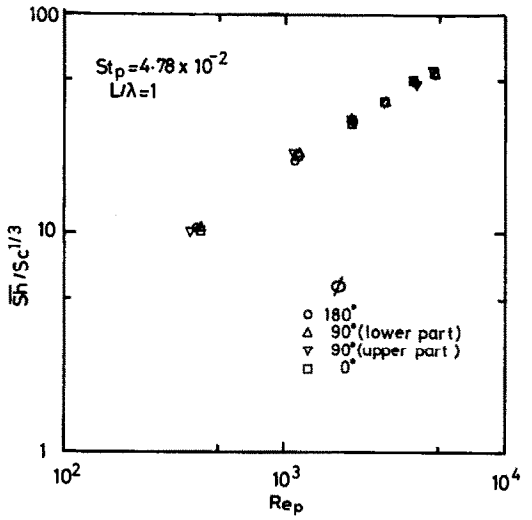

FIG. 12. Effect of ϕ on $\overline{Sh}$.

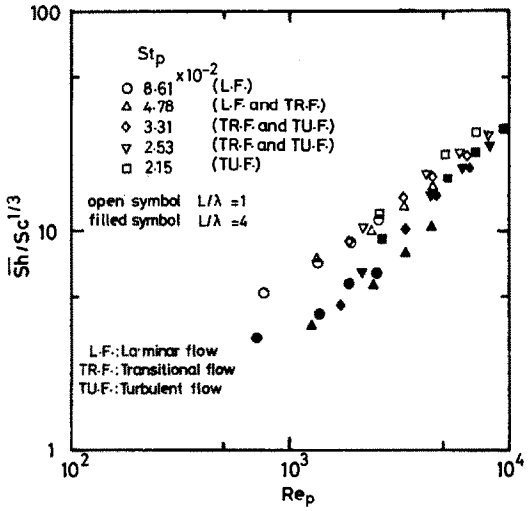

FIG. 14. $\overline{Sh}$ vs Re_p for straight channel.

and the Reynolds number. Open symbols in this figure represent the results of $L/\lambda = 1$ and filled symbols are used for the results of $L/\lambda = 4$. The Sherwood numbers increase with Reynolds number, but the dependence of the Reynolds number changes with the Strouhal number, which is clearly shown at $L/\lambda = 4$. This property is different from that for the wavy channel as shown in Fig. 10. This reason is due to the change of flow pattern as mentioned above. For instance, the mass transfer results for $St_p = 8.61 \times 10^{-2}$ and 2.15×10^{-2} fall down the laminar and turbulent flow regions respectively as additionally noted in this figure. The dependence of the Reynolds number for $St_p = 8.61 \times 10^{-2}$ is smaller than that for $St_p = 2.15 \times 10^{-2}$ from the results at $L/\lambda = 4$. Furthermore, the effect of the mass transfer length is significant, in contrast to the wavy channel case shown in Fig. 11. This reason is deduced from the flow observations that renewal of the concentration boundary layer caused by flow reversal is weaker for the straight channel than for the wavy channel due to no vortex ejection.

4.4. *Mass transfer enhancement*

To examine the enhancement provided by the channel with the wavy wall, the time-averaged Sherwood numbers were compared with those for the channel with straight wall. The condition of comparison is that the height of the straight channel is equal to the average height of the wavy channel, and also that the flow rate and fluid properties are equal, i.e. equal Reynolds number. So the increment in the mass transfer surface for the wavy channel as compared with that for the straight channel (1.14 times) was neglected in this study. The Sherwood number ratio of the wavy channel to the straight channel is plotted against the Reynolds number in Fig. 15 as an example. The Sherwood number ratios are considerably greater than 1 in this experimental range. The results at $St_p = 8.61 \times 10^{-2}$ are larger than those at

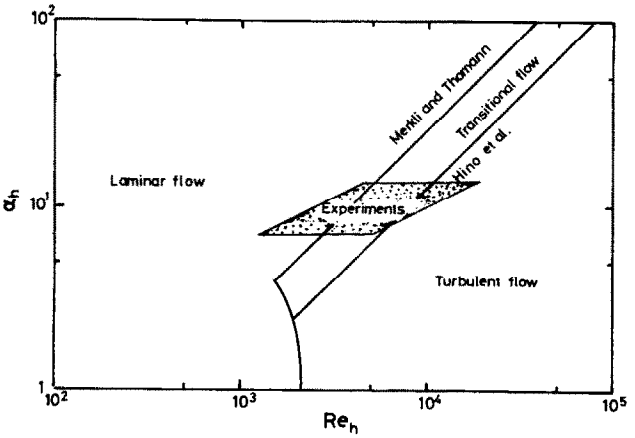

FIG. 13. Flow diagram for straight channel proposed by Ohmi *et al.*

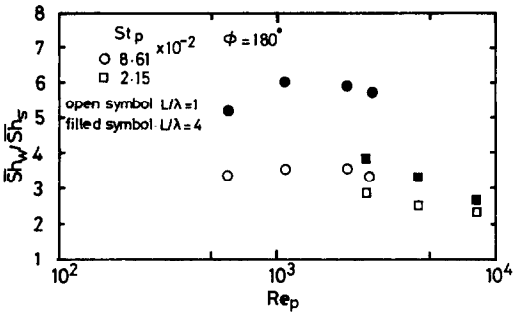

FIG. 15. Comparison of Sherwood numbers for wavy and straight channels.

$St_p = 2.15 \times 10^{-2}$, because the flow conditions for those cases are laminar and turbulent flows in the straight channel, respectively, as mentioned above. Furthermore, the trend of enhancement increases as the value of the mass transfer length increases. The results for $L/\lambda = 4$ indicate a sixfold improvement at the maximum. These results deduce a high efficiency of the membrane oxygenator of Bellhouse *et al.* [1].

5. CONCLUSIONS

Flow and mass transfer characteristics in wavy channels were made clear for oscillatory flow. The experiments were carried out under the following conditions: $5 \times 10^2 < Re_p < 10^4$, $2.1 \times 10^{-2} < St_p < 8.6 \times 10^{-2}$. The wavy channel consists of two sinusoidal wavy plates which can be misaligned by some angle ϕ. Three channel geometries ($\phi = 0$, 90° and 180°) were employed.

In this experimental range, the flow separates during the acceleration phase to form recirculation vortices. During the deceleration phase the vortices grow to fill the entire region of the wavy channel. As the direction of flow reverses, the vortices are ejected from the wall and quickly entrained by the main stream. This property is the same for three wavy channels considered, but the detail of the vortex entrainment process is different.

Time-averaged Sherwood number strongly depends on the Reynolds number, but the effects of the Strouhal number and the mass transfer length are small. These characteristics are the same for the wavy channels considered and also the Sherwood numbers are almost equal to each other.

The mass transfer comparison between the wavy and straight channels under equal mass flow conditions yields large enhancements for the wavy channels, which increase as the mass transfer length is increased. The mass transfer enhancements are attributed to the vortex ejection observed. Those results deduce a high efficiency of membrane oxygenator of Bellhouse *et al.*

In the near future, the detailed mechanism of this enhancement will be considered.

Acknowledgement—The authors acknowledge with thanks the assistance of Messrs Tadashi Yoshino and Shingho Arakawa in the experiments. This work was supported in part by a Grant-in-Aid for Scientific Research (No. 5870092) from the Ministry of Education, Science and Culture of Japan.

REFERENCES

1. B. J. Bellhouse, F. H. Bellhouse, C. H. Curl, T. I. MacMillan, A. J. Gunning, E. H. Spratt, S. B. MacMurray and J. M. Nelems, A high efficiency membrane oxygenator and pulsatile pumping system, and its application to animal trials, *Trans. Am. Soc. artif. internal Organs* **19**, 72–78 (1973).
2. I. J. Sobey, On flow through furrowed channels. Part 1. Calculated flow patterns, *J. Fluid Mech.* **96**, 1–26 (1980).
3. K. D. Stephanoff, I. J. Sobey and B. J. Bellhouse, On flow through furrowed channels. Part 2. Observed flow patterns, *J. Fluid Mech.* **96**, 27–32 (1980).
4. T. Nishimura, Y. Ohori and Y. Kawamura, Flow characteristics in a channel with symmetric wavy wall for steady flow, *J. Chem. Engng Japan* **17**, 466–471 (1984).
5. T. Nishimura, Y. Ohori, Y. Kajimoto and Y. Kawamura, Mass transfer characteristics in a channel with symmetric wavy wall for steady flow, *J. Chem. Engng Japan* **18**, 550–555 (1985).
6. T. Nishimura, Y. Kajimoto and Y. Kawamura, Mass transfer enhancement in channels with a wavy wall, *J. Chem. Engng Japan* **19**, 142–144 (1986).
7. T. Nishimura, Y. Kajimoto, A. Tarumoto and Y. Kawamura, Flow structure and mass transfer for a wavy channel in transitional flow regime, *J. Chem. Engng Japan* **19**, 449–455 (1986).
8. J. K. Aggarwal and L. Talbot, Electro-chemical measurements of mass transfer in semi-cylindrical hollows, *Int. J. Heat Mass Transfer* **22**, 61–75 (1979).
9. T. Mizushina, T. Maruyama, S. Ide and Y. Mizukami, Dynamic behavior of transfer coefficient in pulsating laminar tube flow, *J. Chem. Engng Japan* **6**, 152–159 (1973).
10. P. P. Grassmann and M. Tuma, Applications of the electrolytic method—II. Mass transfer within a tube for steady, oscillating and pulsating flows, *Int. J. Heat Mass Transfer* **22**, 799–804 (1979).
11. S. K. Gupta, R. D. Patel and R. C. Ackerberg, Wall heat/mass transfer in pulsatile flow, *Chem. Engng Sci.* **37**, 1727–1739 (1982).
12. I. J. Sobey, The occurrence of separation in oscillatory flow, *J. Fluid Mech.* **134**, 247–257 (1983).
13. M. Ohmi, M. Iguchi and F. Akao, Laminar–turbulent transition and velocity profiles in rectangular duct for oscillatory flow, *Trans JSME*, Ser. B **49**, 2343–2353 (1983).

CARACTERISTIQUES DE TRANSFERT DE CHALEUR ET DE MASSE DANS LES CANAUX ONDULES POUR UN ECOULEMENT OSCILLANT

Résumé—On étudie l'écoulement oscillant et le transfert massique d'un fluide dans des canaux entre deux plaques ondulées sinusoïdalement. Les expériences ont été conduites dans les conditions suivantes: $5.10^2 < Re_p < 10^4$; $2{,}1.10^{-2} < St_p < 8{,}6.10^{-2}$. L'écoulement est ni dominé par les forces de viscosité, ni par les conditions stationnaires. Le tourbillon de recirculation est formé pendant la phase d'accélération et il est éjecté loin de la paroi après le renversement de l'écoulement. Le transfert de masse dépend fortement de Re_p et l'effet de St_p est insignifiant. Le canal ondulé provoque un accroissement important du transfert de masse en comparaison avec les canaux droits. Cet effet est attribué à l'éjection du tourbillon.

STRÖMUNGS- UND STOFFTRANSPORTEIGENSCHAFTEN OSZILLIERENDER STRÖMUNGEN IN WELLIG GEFORMTEN KANÄLEN

Zusammenfassung—Es wurden die Strömungs- und Transporteigenschaften oszillierender Strömungen in wellig geformten Kanälen, bestehend aus zwei sinusförmig gewellten Platten, untersucht. Die Experimente wurden bei folgenden Versuchsbedingungen durchgeführt: $5 \cdot 10^2 < Re_p < 10^4$, $2{,}1 \cdot 10^{-2} < St_p < 8{,}6 \cdot 10^{-2}$. Die Strömung war bei diesem Experiment weder von den Reibungskräften dominiert noch quasistationär. Der Rückstromwirbel bildet sich in den Vertiefungen während der Beschleunigungsphase und wird unmittelbar nach der Strömungsumkehr von der Wand abgedrängt. Der Stofftransport hängt wesentlich von Re_p ab, der Einfluß von St_p ist vernachlässigbar. Verglichen mit geraden Strömungskanälen ist der Stofftransport in wellig geformten Kanälen stark verbessert. Diese Steigerung wird der Wirbelablösung zugeordnet.

ХАРАКТЕРИСТИКИ ТЕЧЕНИЯ И МАССОПЕРЕНОСА В КАНАЛАХ С ВОЛНООБРАЗНЫМИ СТЕНКАМИ ДЛЯ ПУЛЬСИРУЮЩЕГО ПОТОКА

Аннотация—Исследовались течение жидкости и массоперенос пульсирующего потока в каналах, которые образованы двумя синусоидальными волнообразными пластинами. Эксперименты проводились при $5 \cdot 10^2 < Re_p < 10^4$, $2{,}1 \cdot 10^{-2} < St_p < 8{,}6 \cdot 10^{-2}$. На течение не оказывали влияние вязкостные сила и оно также не являлось квазистационарным. Осциллирующий вихрь образуется на выемке стенки канала в течение ускорения и выталкивается из нее сразу после изменения направления потока. Интенсивность массопереноса сильно зависит от Re_p и незначительно от St_p. Массоперенос в каналах с волнообразными стенками протекает интенсивнее по сравнению с соответствующим гладким каналом. Это увеличение объясняется эжекцией вихрей.